Carbon Nanoparticles for Solar Disinfection of Water

Carbon Nanoparticles for Solar Disinfection of Water

Pratap Reddy Maddigpu[a#], Bhairavi Sawant[b#], Snehal Wanjari[a#], M. D. Goel[a], Davide Vione[c], Rita S. Dhodapkar[b], S. Rayalu[a*]

[a]Environmental Materials Division, CSIR-National Environmental Engineering Research Institute (CSIR-NEERI), Nagpur - 440020, Maharashtra, India.

[b]Waste Water Technology Division, CSIR-National Environmental Engineering Research Institute (CSIR-NEERI), Nagpur - 440020, Maharashtra, India.

[c]Department of Chemistry, University of Torino, Via Pietro Giuria 5, 10125 Torino, Italy.

[*]To whom correspondence should be addressed:
Phone: +91-9890367588; Fax: 0712 – 2247828; E-mail: s_rayalu@neeri.res.in
[#] Equal contribution

Abstract

The present manuscript deals with the application of carbon nano particles (CNP) and chitosan (CHIT) in the form of CHIT-CNP composite for the disinfection of water. The CHIT-CNP composite was prepared by the solution casting method and characterized by TEM, XRD and elemental analysis. In the present investigation we study the disinfection efficiency towards *E. coli* bacteria of both CNP and CHIT-CNP, under sunlight (SODIS) in identical experimental conditions. Both CNP and CHIT-CNP enhanced disinfection as compared to SODIS alone, and comparable performance was achieved when the same dose of CNP in the two materials was applied. However, the CHIT-CNP composite is in the form of a fabric and it is easier to use and handle as compared to the CNP powder, especially in rural and resource-constrained areas. Moreover the SODIS-CHIT-CNP setup, when used in a compound parabolic collector (CPC) reactor showed high bactericidal efficiency compared to SODIS alone, which is promising for practical applications. The disinfection potential of the CNP powder was compared with that of the well-known material TiO_2 Degussa P25 (DP_{25}): DP_{25} gave 6-log kill of bacteria in 180 minutes, whereas CNP produced 6-log kill in 150 minutes.

Keywords : Carbon nanoparticle (CNP); Chitosan-CNP composite; *E. coli*; Water disinfection; SODIS.

1. Introduction

Clean water is necessary to human life and it is a significant feedstock in a variety of industries including pharmaceuticals and food. A recent World Health Organization (WHO) report shows that more than 1.8 billion people in the world do not have access to clean water [1]. As a consequence, water that is highly contaminated with pathogenic organisms is used for drinking purposes. The lack of safe drinking water in developing countries is a continuously growing problem, due to the increase in population and increasing water demand [1]. The main difficulty is presently a lack of water distribution infrastructures and water treatment systems. A literature review has shown that significant progress in water treatment has been made with techniques such as chlorination, ozonation, bioremediation, adsorption processes and photocatalytic oxidation. Moreover, during the past few decades many investigations have been carried out concerning the use of synthetic and natural zeolites, polymer films and metal ions such as Ag, Cu, Zn, Hg, Ti, Ni, Co, Au, Fe as bactericidal agents for water disinfection [2]. The use of nano-catalysts, nano-sorbents, nanostructured catalytic membranes, bioactive nanoparticles, and nanoparticle-enhanced filtration has the potential to solve problems associated with water purification [3-6]. Nanomaterials show promising results because of their high surface area, and the nanomaterials presently used in water treatment can be classified into four groups, i.e., metal-containing nanoparticles (MNP), zeolites, dendrimers and carbon-based nanomaterials. At the same time, nanostructured materials attracted a lot of attention due to their physical, chemical and optical properties [7]. The bactericidal action of several nanoparticles has been well discussed along with merits, limitations and applications for water disinfection and biofouling control [8]. For instance, silver (Ag) nanoparticles can be used conveniently for water

disinfection because the silver ions interact with the thiol groups in the proteins of the bacterial cells, thereby damaging the cell structure [8]. Moreover, the hydroxyl groups occurring on the surface of iron-oxide nanoparticles provide a useful synthetic tool to bind and disperse different functionalities, with promising applications for water disinfection [9].

Metal oxide nanoparticles (MONP) displaying photocatalytic activity are also interesting for water treatment processes. The use of nanoparticles is interesting because they provide an elevated surface area that has important implications on the efficiency of photocatalysis [10]. For instance, zinc oxide nanoparticles provide high surface reactivity linked to the large number of active sites, and they are emerging as efficient nano-photocatalysts as compared to TiO_2 [11]. Silver-loaded titanium dioxide nanoparticles (1wt%Ag-TiO_2) supported on hydroxyapatite (HAP) have been investigated for their capability of disinfecting *E. coli* bacteria in aqueous media [12]. The investigation reported that 5 wt% Ag-TiO_2/HAP was able to kill 100% *E. coli* within 2 minutes. Kaur et al. studied Ag-loaded TiO_2 (1:20, 1:50, 1:100 and 1:200) catalysts prepared by the sol-gel technique, and observed that 1:50 Ag/TiO_2 nanoparticles could disinfect 4.8×10^8 CFU/mL *E. coli* within 60 minutes [13].

Several nanoparticles can thus be applied to water treatment [3], including carbon nanoparticles (CNP). CNP have received considerable attention recently, because their large and hydrophobic surface provides strong adsorption affinity towards a wide range of contaminants. Hence, they can be used as promising adsorbents for the removal of contaminants from water. Besides adsorption, carbonaceous nanomaterials have the potential to purify water through photothermal or photocatalytic properties. The antibacterial activity of carbon nanoparticles is for instance based on their capability to produce photothermal heat when exposed to photon energy (sunlight) [14]. The physical interaction of nanomaterials with bacteria can be crucial for solar disinfection (SODIS) applications. In SODIS,

microbiologically contaminated water is placed in 1-2 L PET (polyethylene terephthalate) bottles and exposed to sunlight for 6 h [15, 16]. The time required for the total disinfection can be significantly shortened with the use of photocatalysts [17, 18], where the interaction between the bacterial cells and the photocatalyst plays an important role in the disinfection mechanism. Carbon-based nanomaterials may cause cell membrane damage in bacteria due to the generation of photothermal heat, with a mechanism that is similar to the destruction of cancerous cells via surface plasmon resonance (SPR) [19].

Solar energy is clean, renewable and abundant, although diluted on a large scale. It is interesting to observe that the sunlight energy incident on Earth is about 1000 times higher than the current world energy consumption. The utilization of the incident sunlight is a feasible solution in everyday practice to obtain clean and safe water, particularly in those rural areas that have availability of prolonged and intense sunlight [20]. For this reason, SODIS is commonly employed in many developing countries as a water treatment technique. Unfortunately, SODIS acts slowly and several proposals have been advanced to accelerate the process, including the use of CNP. Varghese et al. have reported the antibacterial activity of CNP against various pathogenic strains such as the Gram-negative *Proteus refrigere* and *Pseudomonas aeruginosa*, as well as the Gram-positive *Staphylococcus aureus* and *Streptococcus haemolyticus* [21].

Chitosan is used in full-scale water and wastewater treatment systems as a coagulant/flocculant, and it has been recently used as a disinfectant, too [22]. Chitosan has several advantages over other disinfectants because it has a broad spectrum of antimicrobial activity, with high rate of efficiency and low toxicity towards mammalian cells [23]. Venkatesan et al. have synthesized chitosan-carbon nanotube (Chitosan-CNT) hydrogels by the freeze lyophilized method, and they have evaluated antimicrobial activity against *Staphylococcus aureus, Escherichia coli* and *Candida tropicalis* [24].

In the present investigation we used a cost-effective method to synthesize carbon nanoparticles (CNP), and fabricated a sheet of composite material containing chitosan (CHIT) together with CNP. We then tested the solar disinfection performance of CNP and a CHIT-CNP composite in batch conditions and in a Compound Parabolic Collector (CPC) reactor. To the best of our knowledge, this is the first report of the use of a Chitosan (CHIT) – CNP composite fabric membrane in the context of SODIS. The studied technique is interesting because it may provide a low-cost and easy-to-operate system for the solar disinfection of microorganisms in water, exploiting the synergistic bactericidal activity of CNP and Chitosan.

2. Experimental

2.1. Materials and chemicals

Chitosan, having 95% deacetylation degree (DD) and molecular weight (MW) of 360 kDa was purchased from Chemchito India Limited, Chennai (India). Soybean oil used as CNP precursor was purchased from the local market and it was used as provided, without any further purification. Titanium dioxide P_{25} (DP_{25}) was obtained from Degussa AG, Germany, and it was used as a benchmark photocatalyst for the assessment of the disinfection rates. All the other chemicals including glacial acetic acid (99.8%) were purchased from Merck, India. The well water (WLW) used had a natural pH of 7.5 -7.9, turbidity lower than 15 NTU and relatively low organic content (chemical oxygen demand of 18-25 O_2 mg/L).The characteristics of the well water are provided in Table 1, and this water was used throughout the experiments.

2.2. Synthesis of CNP and CHIT-CNP composite film

The synthesis of Carbon Nanoparticles (CNP) was carried out as per the method reported by Rayalu et al. [25]. In a typical procedure, a cotton wick was soaked in oil for a certain time period and then it was burned at room temperature in a traditional *vedic* lamp.

The generated carbon nanoparticles (CNP) were collected over a brass plate that was held at a fixed position over the lamp. The synthesized nanoparticles were used as such for the solar disinfection of *E.coli*, without further purification. It was found that the morphology and size of the recovered CNP was highly dependent on the size of the wick and the distance of the brass plate from the lamp. This distance was thus maintained in such a way that the collected CNP has sizes in the range of 30 to 35 nm. The CHIT-CNP membrane was prepared by dissolving different doses (2-10 mg) of the CNP powder in 10 mL of chitosan (CHIT) solution (3% w/v), stirring for an hour. Air bubbles were removed by centrifugation, after which the suspension was slowly spread on a glass plate and dried at room temperature to allow the development of the composite CHIT-CNP film.

2.3. Characterization of materials

The prepared CNP and the CHIT-CNP composite were characterized by X-ray diffraction (XRD), transmission electron microscopy (TEM), UV-vis and IR spectroscopy, as well as elemental analysis according to the procedures described in the supplementary material **S.**

2.4. Antimicrobial activity

2.4.1. Bacterial Strain and cultivation

The *E. coli* ATCC 25922 bacterial strains used in the present investigation were received from CSIR-Institute of Microbial Technology (CSIR-IMTECH), Chandigarh, India. Bacterial cultures were obtained by streaking the freezing stock (stored at -20 to -80°C) onto nutrient agar plates (HIMEDIA, Mumbai, India) that were incubated for 24 h at 37°C. A single colony was then inoculated into a 10 mL sterilized nutrient broth (HIMEDIA, Mumbai, India) and incubated on rotary shaker for 18 h at 37°C. Bacterial cells were harvested by centrifuging the above broth at 3000rpm for 15 minutes. The obtained pellet was suspended in 10 mL sterilized phosphate buffer saline (PBS) to obtain a final

concentration of 10^9 CFU (colony forming units)/mL. A suitable volume of this PBS solution was spiked in experimental well water (WLW) in order to obtain 10^6 CFU/mL as the starting concentration of bacteria. One mL of the sample was used after consecutive dilutions to achieve a countable population of bacteria on a Petri dish. Each sample was plated in triplicate after suitable serial dilutions, and the colony-forming units (CFU/mL) were counted following 24 h incubation at 37°C.

2.4.2. Solar experiments – Effect of CNP dose as standalone CNP suspension and as dose in CHIT-CNP composite film

All the experiments were performed in borosilicate glass beakers (100 mL) with UV-A transparent borosilicate glass covers (300-nm cut-off wavelength) in the month of September, 2014, at Nagpur, India (21.15°N, 79.09°E). Well water (WLW) spiked with *E. coli* ATCC 25922 was used throughout the investigation. Thereafter, WLW was spiked with *E. coli* as described above, aerated for 10 min to dissolve air and exposed directly to sunlight for SODIS control experiments. Table 1 shows the physico-chemical parameters of the WLW before and after the treatment. The table shows that the treatment in the presence of CNP did not cause important changes in the WLW parameters, which was also true for the SODIS treatment alone (without CNP).

In the CNP experiments, the CNP dose was varied in the range of 2-50mg CNP per 50 mL of WLW, and 1 mL sample aliquots were withdrawn after suitable time intervals for bacteria enumeration. In order to determine the CNP bactericidal efficiency under sunlight, the CNP performance was compared with that of the commercially available DP_{25} photocatalyst. This TiO_2 material contains anatase and rutile phases in a ratio of about 3:1, and it has been used by several researchers for photocatalytic oxidation and disinfection. For the DP_{25} experiments we used 10 mg of DP_{25} dispersed in 50 mL WLW spiked with *E. coli*

ATCC 25922, exposing this system to sunlight and following the same experimental procedure as for CNP.

Further, the CHIT-CNP composite was prepared as described in section 2.2. The CHIT-CNP membranes thus obtained were placed vertically in 100 mL beakers containing 50 mL WLW spiked with *E. coli* ATCC 25922, and the beakers where then exposed to sunlight as described above. Blank experiments were simultaneously performed in the dark in otherwise identical experimental conditions, and in these dark experiments the enumeration of bacteria was carried out at the end of each experimental run.

Further experiments were carried out by using a CPC reactor as a ONE SUN solar radiation collector (Fig. 1a). The CPC reactor consisted of four inner tubes coated with immobilized CNP material (CHIT-CNP composite film) on their external surface (Fig. 1c). These coated tubes were placed concentrically inside the outer tubes (Fig. 1b), where the treatment water was circulated as shown in Fig. 1a. Therefore, the CHIT-CNP film wrapped around the inner tubes was in contact with the treatment water circulating inside the outer tubes. The CPC reactor was operated in recirculating mode with the help of a peristaltic pump. Blank experiments were also performed in the CPC reactor without the CHIT-CNP composite film coating, for comparison of the efficiency.

2.4.3. Disinfection Kinetics

The Chick and Watson disinfection model was used to calculate the disinfection kinetics. This model is based on pseudo-first order reaction kinetics and the relevant equation reads as follows:

$$\log\left(N/N_0\right) = -kt$$

where N is the concentration of viable microorganisms at time 't', N_0 their initial concentration, and k the disinfection rate constant. This law is respected if, under constant

irradiation conditions within the same reactor, the concentration of disinfecting agent is approximately constant over time for a fixed catalyst concentration [26].

2.4.4. Measurement of UV Radiation and Temperature

The intensity of UVA radiation was measured using a UV radiometer (ILT 1700 Research radiometer, NIST Traceable Light measurement) with detector model no. SED240. The temperature measurement was carried out using a thermometer immersed in the solution.

3. Results and Discussion

3.1. Characterization of CNP

3.1.1. XRD, TEM, UV-vis spectroscopy and Elemental analysis

The XRD pattern of synthesized CNP is shown in Fig. S1 (supplementary material). From the Figure, it is clear that there are two broad peaks near $2\theta = 23.68°$ and 44.01°. Both peaks suggest the occurrence of amorphous material and are evidence of high-quality carbon nanomaterials [25]. Moreover, the TEM image of CNP (Fig. S2) shows particles size, morphology and structural details. The micrograph reveals the presence of interconnected carbon particles that form elongated spherules. These spherules are expected to produce improved electron transport and to help the localization of the substrate [27]. The average particles were in the range of 30-50 nm with irregular morphology. From the elemental analysis, carried out on a Variol EL III CHNS analyzer, it was found that CNP contain 91% elemental C, 0.053% H, 0.045% N and no S. The UV-visible spectrum of CHIT-CNP shows a broad-band absorption from 300 to 700 nm (Fig. S3). The increase of the absorbance in the visible region by CHIT-CNP compared to CNP suggests that, in agreement with previous reports concerning carbon black absorption properties [28], the composite carbon film might be capable of exploiting solar radiation for disinfection.

3.1.2. Infra-red spectroscopy analysis of CHIT and CHIT-CNP composite

IR spectra were recorded of the freshly prepared CHIT film, fresh CHIT-CNP film and used CHIT-CNP film (Fig. 2). The bands in the IR spectrum of CHIT in the range from 3750 to 3000 cm^{-1} can be attributed to the stretching vibrations of the OH groups, which partially overlap with the stretching vibrations of the C-H bond in the $–CH_2$ (2961 cm^{-1}) and $–CH_3$ (2846 cm^{-1}) groups, respectively [29]. Bending vibrations of the methyl and methylene groups are also visible at 1375 cm^{-1} and 1426 cm^{-1}, respectively. Absorption at 1680–1480 cm^{-1} is related to the vibrations of the carbonyl bond (C=O) of the amide group CONHR (secondary amide, centered at 1647cm^{-1}) and to the vibrations of the protonated amine group (1566 cm^{-1}) [30]. Absorption in the range from 1158 cm^{-1} to 1000 cm^{-1} is due to the vibrations of the CO group. The band located near 1158 cm^{-1} corresponds to the asymmetric vibrations of CO in the oxygen bridge resulting from the deacetylation of CHIT. The bands near 1080–1025 cm^{-1} are attributed to the stretching vibration of CO in the ring groups COH, COC and CH_2OH [31]. The small peak at 890 cm^{-1} corresponds to the saccharide structure (wagging) of CHIT [30].

FT-IR was also used to study the CHIT/CNP interaction, because a shift in the protonated amino group vibration might be expected when $–NH_3^+$ interacts electrostatically with the negatively charged sites of CNP. These results are in agreement with the findings reported in the literature [29-33]. The composite CHIT-CNP structure enables an electron exchange between CNP and the functional groups of CHIT, thereby allowing redox reactions [34]. In Fig. 3 it is provided the comparative FT-IR spectrum of fresh CHIT-CNP, and of the CHIT-CNP film exposed for 90 min under solar light in the presence of the treatment water in the compound parabolic collector (CPC) reactor. The spectra show a broad absorption signal from 3000 to 3500 cm^{-1} due to the stretching vibrations of the NH_2 and OH groups, which was drastically decreased upon exposure to sunlight in the CPC reactor. This decrease

suggests that a modification of CHIT under irradiation would take place, and that it would mainly involve the groups NH_2 (coherently with their interaction with CNP) and OH.

3.2. Antimicrobial Studies

3.2.1. Effect of Solar Radiation and CNP Dose

In SODIS experiments, the inactivation of bacteria is due to the synergistic effect of the 3-5% UV-A radiation and the thermal energy in the solar spectrum [35]. In our experiments, when natural well water containing bacteria was exposed continuously to sunlight for about 5.5 - 6 h, a 6-log kill was achieved. The well water we used had a natural pH of 7.5 -7.9, turbidity lower than 15 NTU and a low organic content in terms of chemical oxygen demand (18-25 mg O_2 /L). The characteristics of well water are given in Table 1 and this same water was used throughout the experiments. A number of organic and inorganic species present in water (chloride, arsenic, nitrate, nitrite, NOM, pesticides etc.) have shown detrimental effects on the rate of disinfection in both SODIS and photocatalytic experiments [36]. The ability of CNP to kill bacteria under irradiation was ascertained in an initial experiment in beakers as described in the experimental section. The solar radiation intensity was measured, because the irradiance of sunlight varies significantly due to daily weather and solar zenith angle conditions.

Fig. 4 shows the effect of the variation of the CNP dose on the rate of disinfection, by reporting the trends of bacteria inactivation with time. The irradiance of sunlight was comparable in all the experiments conducted. It can be observed from the figure that disinfection was considerably improved in the presence of the suspended CNP powder, and a 6-log kill could be achieved in less than 75 min in the presence of a CNP dose higher than 25 mg/50 mL. For a comparison with blank runs, exposure to CNP for 90 minutes in the dark resulted in just 10-50% reduction in the bacterial colony-forming units.

The curves shown in Fig. 4 have a log-linear inactivation region and a final tail also termed as the deceleration process, in agreement with previous reports [37]. The majority of the disinfection occurred in the first linear phase, which was thus taken into account to calculate the disinfection rate. The addition of CNP clearly improved the SODIS disinfection, and the cumulative UVA dose needed to achieve a 6-log reduction value was, on the average, 198 kJ and 58 kJ for SODIS experiments carried out without and with 25 mg/50 mL suspended CNP, respectively. The temperature at the end of the SODIS experiments was 44°C with CNP and 53°C without CNP. Therefore, the solution temperature does not appear to play a major role in bacterial inactivation in the present experiments, but there is also evidence that carbon-based nanomaterials are able to generate reactive oxygen species that can carry out a cytotoxic action [38].

In order to investigate the effect of dose variation and to compute the optimum one, the dose of CNP powder added to well water (WLW) spiked with *E. coli* was varied in the range of 2-50 mg/50 mL. The suspensions thus obtained were exposed to direct sunlight with continuous stirring during the month of September, 2014, in Nagpur, India (21.15°N, 79.09°E). The samples were withdrawn at 10 min intervals for the enumeration of *E. coli.* All experiments were carried out in triplicates and repeated on three days during the month. Table 2 shows the disinfection kinetics data for the studied CNP doses, as well as the results obtained with SODIS alone without CNP. An increase in disinfection rate was observed with the increase in the dose of CNP, and optimum conditions (i.e., a dose for which the disinfection rate was maximum) were not identified in the studied dose range. Interestingly, CNP at 25 mg/50 mL dose attained complete disinfection in 75 min exposure time, and the relevant disinfection rate was found to be enhanced by 3.2 times in comparison with SODIS alone, without CNP. The time needed to obtain a 6-log kill varied from 120 min at a dose of 5 mg/50 mL to 60 min at a dose of 50 mg/50 mL. However, a dose of 25 mg/50 mL can

achieve 99% absorption of the solar radiation ($\lambda > 300$ nm) entering the photo-reactor, and it can be considered as satisfactory for disinfection.

Further experiments were carried out with the composite material CHIT-CNP, added to WLW spiked with *E. coli*. In this case the doses of CNP in the CHIT-CNP composite were varied from 2 mg/50 mL to 10 mg/50 mL, and a 6-log kill was obtained in 90 minutes of sunlight exposure in the presence of 10 mg/50 mL of CNP in CHIT-CNP (see Table 3 and Fig. 5). In the same conditions, the temperature increased from 23°C to 41°C in 90 min as reported in Table 3. At a dose of 5 mg/50 mL the time to achieve a 6-log kill was 120 min, as compared with 90 min for 10 mg/50 mL. Therefore, a dose of 10 mg/50 mL can be considered as the best option for CHIT-CNP. For comparison with the blank runs, exposure to CHIT-CNP in the dark for 150 min produced a decrease of just 2-21.15 % in the bacterial colony forming units.

When comparing the efficiencies of the CNP powder and the CHIT-CNP composite, it is observed that the CNP powder under optimal conditions (6-log reduction in 75 minutes at 25 mg/50 mL) showed a somewhat higher efficiency than the CHIT-CNP composite (6-log reduction in 90 minutes at 10 mg/50 mL). However, CHIT-CNP at 10 mg/50 mL CNP dose showed comparable performance as CNP at 10 mg/50 mL, and similar findings were obtained whenever CNP and CNP in CHIT-CNP were used at the same dose (see Table 2 and Table 3). On the one side, it is to be noted that CNP immobilized in CHIT has less contact with WLW as compared to CNP dispersed throughout the WLW volume. On the other side, CHIT is known to have an anti-microbial action on its own [22] that would be added to the anti-microbial performance of CNP. Moreover, considering that CHIT-CNP is in the form of a tissue, it is easier to use in practical applications than a CNP water suspension (*vide infra*).

3.2.2. Comparison of DP_{25} and CNP powder

The DP_{25} material is used as a standard for disinfection in SODIS conditions [39]. A single dose of DP_{25} (10 mg/50 mL) and two doses of CNP powder (10 mg/50 mL and 50 mg/50 mL) were spiked to WLW, and the different systems were exposed to sunlight (SODIS). The temperature increased to 48°C and 52°C from 23°C for DP_{25} and the CNP powder, respectively. Fig. 6 and Table 3 show the results of irradiation experiments for DP_{25}, for CNP at the two doses (the 10 mg/50 mL one is shown in Fig. 6), and for SODIS alone. The relevant disinfection rate constants were 0.019 min^{-1} (SODIS), 0.032 min^{-1} (DP_{25}), 0.040 min^{-1} (CNP at 10 mg/50 mL), and 0.119 min^{-1} (CNP at 50 mg/50 mL). These results indicate that, depending on the CNP dose, the disinfection rate constant was enhanced in the presence of CNP by 2 to 6 times compared to SODIS alone. Moreover, a 6-log kill was achieved in 300 min (SODIS), 180 min (DP_{25}), 150 min (CNP at 10 mg/50 mL), and 60 min (CNP at 50 mg/50 mL). These results confirm the effectiveness of CNP for water disinfection and suggest that, in the SODIS context, CNP shows comparable disinfection capability as DP_{25}.

3.2.3. Compound parabolic collector (CPC) reactor study

In order to check for the efficiency of the used approach in conditions that are nearer to practical applications, and to understand the effect of water recirculation, another set of experiments was carried out using a Compound Parabolic Collector (CPC) reactor (Fig.1). The CPC reactor was operated in recirculating mode and the flow rate was 28 mL/min at 42 rpm. In the reactor, WLW and CHIT-CNP composite coat film were used for performance investigation. The disinfection rate constant based on the Chick-Watson model was found to be k = 0.008 min^{-1} for CPC:SODIS alone, and k = 0.037 min^{-1} for CPC:SODIS-CHIT-CNP (Table 4). The time evolution of the two systems is shown in Fig. 7, in which one can see that CPC:SODIS-CHIT-CNP achieved 6-log kill in 180 minutes whereas CPC:SODIS took over 300 min to achieve a 5-log kill. The higher disinfection shown by CPC:SODIS-CHIT-CNP

compared to CPC:SODIS is likely due to the synergistic effect of the antibacterial activities of CHIT and CNP.

4. Conclusion

This study presents a novel approach to use a CHIT-CNP composite membrane against *Escherichia coli* under solar irradiation, showing highly efficient antimicrobial activity when used in a recirculating compound parabolic collector (CPC) reactor. The latter is a similar system as those used in practical applications. Characterization of CNP was done successfully by TEM, XRD and elemental analysis. The batch study of antimicrobial activity showed that CNP and CHIT-CNP performed better than solar irradiation (SODIS) alone. The disinfection kinetics by both CNP and CHIT-CNP was strongly dose-dependent, and the disinfection rate constant continuously increased when increasing the CNP dose (either suspended or incorporated inside the CHIT film). Comparable results in terms of both rate constants and times needed to achieve a 6-log kill of bacteria were obtained when equal doses of CNP were used in the form of suspended powder or inside the CHIT-CNP composite film. On the one side, it could be expected that CHIT-immobilized CNP is less effective than the CNP powder towards bacteria inactivation. However, in the case of the CHIT-CNP composite there is a likely synergic effect of the two components towards bacteria inactivation, because CHIT is known to have bactericidal activity, too. Interestingly, CNP under sunlight irradiation showed similar and even slightly higher bactericidal performance than the widely studied photocatalyst DP_{25} in comparable experimental conditions. The main advantage of CHIT-CNP as compared to the CNP powder lies in the fact that CHIT-CNP has a tissue form that allows its use in practical applications. For instance, CHIT-CNP could be wrapped around the inner CPC reactor tube as the treatment water flowed in the outer tube, which would not be possible by using the CNP powder. In the CPC reactor case also, CHIT-CNP enhanced disinfection as compared to SODIS alone.

Acknowledgments

The communicating author acknowledges the funding and support received from CSIR under CoE-MESER (ESC-0108) project for completing the reported investigation. Dr. Maddigapu Pratap Reddy thanks CSIR, New Delhi in granting the CSIR-NEERI Pool Scientist award.

References:

[1] WHO/UNICEF Joint Monitoring Programme for Water Supply, Sanitation and Hygiene (JMP)-2016 (http://www.unwater.org/publication_categories/whounicef-joint-monitoring-programme-for-water-supply-sanitation-hygiene-jmp/)

[2] P. Jain, T. Pradeep, Potential of silver nanoparticle-coated polyurethane foam as an antibacterial water filter. Biotechnol. Bioeng. 90 (2005) 59-63.

[3] T.E.A. Chalew, G.S. Ajmani, H. Huang, K.J. Schwab, Evaluating nanoparticle breakthrough during drinking water treatment. Environ. Health Perspect. 121 (2013) 1161–1166.

[4] X. Zhang, T. Zhang, J. Ng, D.D. Sun, High-performance multifunctional TiO_2 nanowire ultrafiltration membrane with a hierarchical layer structure for water treatment. Adv. Funct. Mater. 19 (2009) 3731-3736.

[5] A. Alonso, X.M. Berbel, N. Vigués, R.R. Rodríguez, J. Macanás, M. Muñoz, J. Mas, D.N. Muraviev, Superparamagnetic Ag@Co-nanocomposites on granulated cation exchange polymeric matrices with enhanced antibacterial activity for the environmentally safe purification of water. Adv. Funct. Mater. 23 (2013) 2450-2458.

[6] P. Xu, G.M. Zeng, D.L. Huang, C.L. Feng, S. Hu, M.H. Zhao, C. Lai, Z. Wei, C. Huang, G.X. Xie, Z.F. Liu, Use of iron oxide nanomaterials in wastewater treatment: A review. Sci. Total Environ. 424 (2012) 1-10.

[7] G.M. Rios, Nanotechnologies and membrane engineering at the core of water and related questions in the Mediterranean and Middle-East countries. In: M.E. Moujabber, L. Mandi, G.T. Liuzzi, I. Martin, A. Rabi, R. Rodriguez (Eds.), Technological perspectives for rational use of water resources in the Mediterranean region. Options Madeterraneennes, series A, 88, CIHEAM, Bari, Italy, 2009, pp. 141-148.

[8] Q. Li, S. Mahendra, D.Y. Lyon, L. Brunet, M.V. Liga, D. Li, P.J.J. Alvarez, Antimicrobial nanomaterials for water disinfection and microbial control: potential applications and implications. Water Res. 42 (2008) 4591-4602.

[9] P.N. Dave, L.V. Chopda, Application of iron oxide nanomaterials for the removal of heavy metals. J. Nanotechnol. 2014 (2014) 1-14.

[10] X. Wang, Y. Du, L. Fan, H. Liu, Y. Hu, Chitosan- metal complexes as antimicrobial agent: Synthesis, characterization and structure-activity study. Polym. Bull. 55 (2005) 105-113.

[11] S. Baruah, S.K. Pal, J. Dutta, Nanostructured zinc oxide for water treatment. Nanosci. Technol.-Asia 2 (2012) 90-102.

[12] M.P. Reddy, A. Venugopal, M. Subrahmanyam, Hydroxyapatite-supported Ag–TiO_2 as *Escherichia coli* disinfection photocatalyst. Water Res. 41 (2007) 379- 386.

[13] P. Kaur, A. Choudhary, R. Thakur, Synthesis of chitosan-silver nanocomposites and their antibacterial activity. Int. J. Sci. Eng. Res. 4 (2013) 869-872.

[14] X. Liu, M. Wang, S. Zhang, B. Pan, Application potential of carbon nanotubes in water treatment: A review. J. Environ. Sci. 25 (2013) 1263-1280.

[15] R. Meierhofer, M. Wegelin, Solar water disinfection - A guide for applications of SODIS, Eawag-Sandec report No. 06/02, Duebendorf, Switzerland, 2002, pp. 1-88.

[16] M.B. Keogh, M. Castro-Alférez, M.I. Polo-López, I.F. Calderero, Y.A. Al-Eryani, C. Joseph-Titus, B. Sawant, R. Dhodapkar, C. Mathur, K.G. McGuigan, P. Fernández-Ibáñez, Capability of 19-litre polycarbonate plastic water cooler containers for efficient solar water disinfection (SODIS): field case studies in India, Bahrain and Spain. Sol. Energy 116 (2015) 1-11.

[17] T. Zhang, X. Wang, X. Zhang, Recent progress in TiO_2-Mediated solar photocatalysis for industrial wastewater treatment. Int. J. of Photo Energy 2014 (2014) 10-12.

[18] S. Malato, P. Fernández-Ibáñez, M.I. Maldonado, J. Blanco, W. Gernjak, Decontamination and disinfection of water by solar photocatalysis: Recent overview and trends. Catal. Today 147 (2009) 1-59.

[19] O. Neumann, C. Feronti, A.D. Neumann, A. Dong, K. Schell, B. Lu, E. Kim, M. Quinn, S. Thompson, N. Grady, P. Nordlander, M. Oden, N.J. Halas, Compact solar autoclave

based on steam generation using broadband light-harvesting nanoparticles. Proc. Natl. Acad. Sci. 110 (2013) 11677-11681.

[20] M. Wegelin, S. Canonica, K. Mechsner, T. Fleischmann, Solar water disinfection: Scope of the process and analysis of radiation experiments. J. Water Supply Res. Technol. Aqua 43 (1994) 154-169.

[21] S. Varghese, S. Kuriakose, S. Jose, Antimicrobial activity of carbon nanoparticles isolated from natural sources against pathogenic gram-negative and gram-positive bacteria. J. Nanosci. 2013 (2013) 1-5.

[22] E.I. Rabea, M.E.-T. Badawy, C.V. Stevens, G. Smagghe, W. Steurbaut, Chitosan as antimicrobial agent: applications and mode of action. Biomacromolecules 4 (2003) 1457-1465.

[23] M. Kong, X. G. Chen, K. Xing, H. J. Park, Antimicrobial properties of chitosan and mode of action: A state of the art review. Intern. J. Food Microbiol. 144 (2010) 51-63.

[24] J. Venkatesan, R. Jayakumar, A. Mohandas, I. Bhatnagar, S.K. Kim, Antimicrobial activity of chitosan-carbon nanotube hydrogels. Materials 7 (2014) 3946-3955.

[25] S.S. Rayalu, J.V. Meenal, M.A. Priti, T.A. Jayshri, N.K. Labhsetwar, S.R. Wate, 0216DEL2012, India patent.

[26] H. Lebik, F. Madjene, L. Aoudjit, S. Igoud, Modelling the kinetic of UV water disinfection. Int. J. Sci. Res. Manage. Stud. 1 (2014) 60-64.

[27] S.C. Ray, A. Saha, N.R. Jana, R. Sarkar, Fluorescent carbon nanoparticles: synthesis, characterization and bioimaging application. J. Phys. Chem. C, 113 (2009) 18546-18551.

[28] D.X. Han, Z.G. Meng, D.X. Wu, C.Y. Zhang, H.T. Zhu, Thermal properties of carbon black aqueous nanofluids for solar absorption. Nanoscale Res. Lett. 6 (2011) 457.

[29] J.F. Mano, D. Koniarova, R.L. Reis, Thermal properties of thermoplastic starch/synthetic polymer blends with potential biomedical applicability. J. Mater. Sci. - Mater. Med. 14 (2003) 127-135.

[30] R.H. Marchessault, F. Ravenelle, X.X. Zhu, Polysaccharides for drug delivery and pharmaceutical applications. A.C.S. symposium series 934, 2006. DOI: 10.1021/bk-2006-0934.fw001.

[31] Y. Xu, K. Kim, M. Hanna, D. Nag, Chitosan-starch composite film: preparation and characterization. Ind. Crop. Prod. 21 (2005) 185-192.

[32] C. Paluszkiewicz, E. Stodolak, M. Hasik, M. Blazewicz, FT-IR study of montmorillonite–chitosan nanocomposite materials. Spectrochim. Acta, Part A 79 (2011) 784-788.

[33] Q. Yuan, J. Shah, S. Hein, R.D.K. Misra, Controlled and extended drug release behavior of chitosan-based nanoparticle carrier. Acta Biomaterialia 6 (2010) 1140-1148.

[34] H. Wang, Y. Wu, P. Wu, S. Chen, X. Guo, G. Meng, B. Peng, J. Wu, Z. Liu, Environmentally benign chitosan as reductant and supporter for synthesis of Ag/AgCl/chitosan composites by one-step and their photocatalytic degradation performance under visible-light irradiation. Frontiers of Materials Science, 11 (2017) 130-138

[35] P.S.M. Dunlop, M. Ciavola, L. Rizzo, J.A. Byrne, Inactivation and injury assessment of *Escherichia coli* during solar and photocatalytic disinfection in LDPE bags. Chemosphere 85 (2011) 1160-1166.

[36] D.M.A. Alrousan, P.S.M. Dunlop, T.A. McMurray, J.A. Byrne, Photocatalytic inactivation of *E. coli* in surface water using immobilised nanoparticle TiO_2 films. Water Res. 43 (2009) 47-54.

[37] K. M. Garza, K. F. Soto, L. E. Murr, Cytotoxicity and reactive oxygen species generation from aggregated carbon and carbonaceous nanoparticulate materials. Int. J. Nanomedicine 3 (2008) 83-94.

[38] P.C. Maness, S. Smolinski, D.M. Blake, Z. Huang, E.J. Wolfrum, W.A. Jacoby, Bactericidal activity of photocatalytic TiO_2 reaction: toward an understanding of its killing mechanism. Appl. Environ. Microbiol. 65 (1999) 4094-4098.

Tables

Table 1 Characterization of well water before and after the solar disinfection treatment

Sr. No.	Parameters	Well Water	
		Before	After
1	pH	7.9	8
2	Conductivity (µmol/cm)	315	320
3	COD (mg/L)	23	20
4	Chloride (mg/L)	18	20
5	Alkalinity (mg/L)	318	300
6	Turbidity (NTU)	15	10

Table 2 Decay rates and 6-log reduction for CNP

CNP Dose, mg/50mL	LRV 6 time (min)	$T_{(min.)}$ (°C)	$T_{(max.)}$ (°C)	Average UV-A Dose (kJ/m^2)	Final CFU/mL	Decay Rates k_t (min^{-1})	R^2
0	240	20-23	53±2.5	198.79	9±5	0.024	0.952
2	>150	20-23	40±1.5	118.53	29±10	0.035	0.907
3	>150	20-23	40±1.5	118.53	22±10	0.036	0.915
4	150	20-23	43±3.5	118.53	14±10	0.037	0.929
5	120	20-23	43±4.5	100.71	2±5	0.049	0.944
10	120	20-23	40±4.5	100.71	1±5	0.054	0.983
25	75	20-23	44±4.5	58.29	5±5	0.096	0.918
50	60	20-23	43±4.5	37.13	5±5	0.119	0.906

"LRV 6": 6-Log Reduction Value; Initial CFU/mL value is 10^6

Table 3 Decay rates and 6-log reduction for DP_{25} and CNP

DP_{25} and CNP	LRV 6 time (min)	$T_{(min.)}$ (°C)	$T_{(max.)}$ (°C)	Average UV-A Dose ($kJ\text{-}m^2$)	Final CFU/mL	Decay Rates k_t (min^{-1})	R^2
SODIS	300	20-23	53±2.5	229.65	7±5	0.019	0.864
DP25 (TiO_2) (10mg/50mL)	180	20-23	48±2	151.96	2±5	0.032	0.953
CNPs (10mg/50mL)	150	20-23	52±2	127.16	5±5	0.040	0.923
CNPs (50mg/50mL)	60	20-23	43±4.5	37.13	5±5	0.119	0.906

Initial CFU/mL value is 10^6

Table 4 Decay rates and 6-log reduction for CNP in CHIT-CNP composite film. The dose is referred to CNP inside the CHIT-CNP composite material

CHIT-CNP Dose, mg/50mL	LRV 6 time (min)	$T_{(min.)}$ (°C)	$T_{(max.)}$ (°C)	Average UV-A Dose (kJ/m^2)	Final CFU/mL	Decay Rates k_t (min^{-1})	R^2
0	240±30	20-23	53±2.5	198.79	9±5	0.024	0.952
2	>150	20-23	42±1.5	118.53	37±10	0.036	0.897
3	>150	20-23	42±1.5	118.53	32±10	0.037	0.929
4	>150	20-23	42±3.5	118.53	29±10	0.038	O.914
5	120±10	20-23	41±4.5	100.71	15±5	0.044	0.926
10	90±5	20-23	41±4.5	80.25	1±5	0.049	0.959
CHIT Blank	>150	20-23	49±15	99±5	8±2	0.030	0.897

Initial CFU/mL value is 10^6

Figure Captions

Figure number	Figure caption
Fig. 1.	(a and b) Compound Parabolic Collector (c) inner tube coated with CHIT- CNP composite film
Fig. 2.	FT-IR spectra of fresh CHIT, fresh CHIT/CNP composite film and used CHIT/CNP composite film
Fig. 3.	FTIR spectra of CHIT-CNP before solar illumination and after solar illumination
Fig. 4.	Solar disinfection (SODIS) of *E. coli* with time Vs concentration of CNP
Fig. 5.	Solar disinfection (SODIS) of *E. coli* with time Vs concentration of CNP in CHIT-CNP composite film
Fig. 6.	Solar disinfection (SODIS) of *E. coli*: Comparative study-CNP with DP_{25}
Fig. 7.	Solar disinfection (SODIS) of *E. coli* with time in Compound Parabolic Collector (CPC) reactor: with CHIT-CNP and without CHIT-CNP (SODIS alone)

00

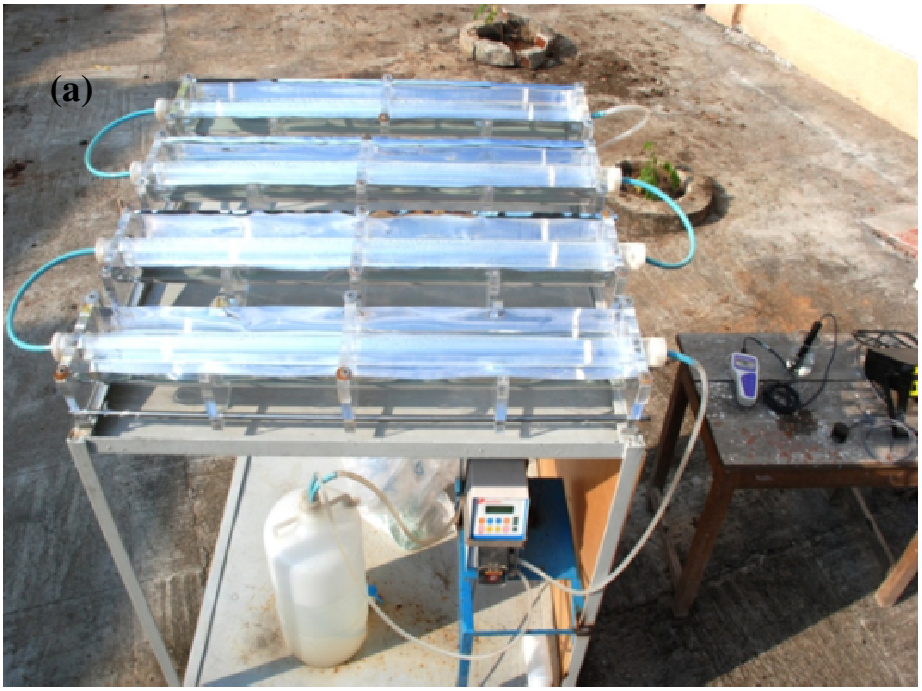

00

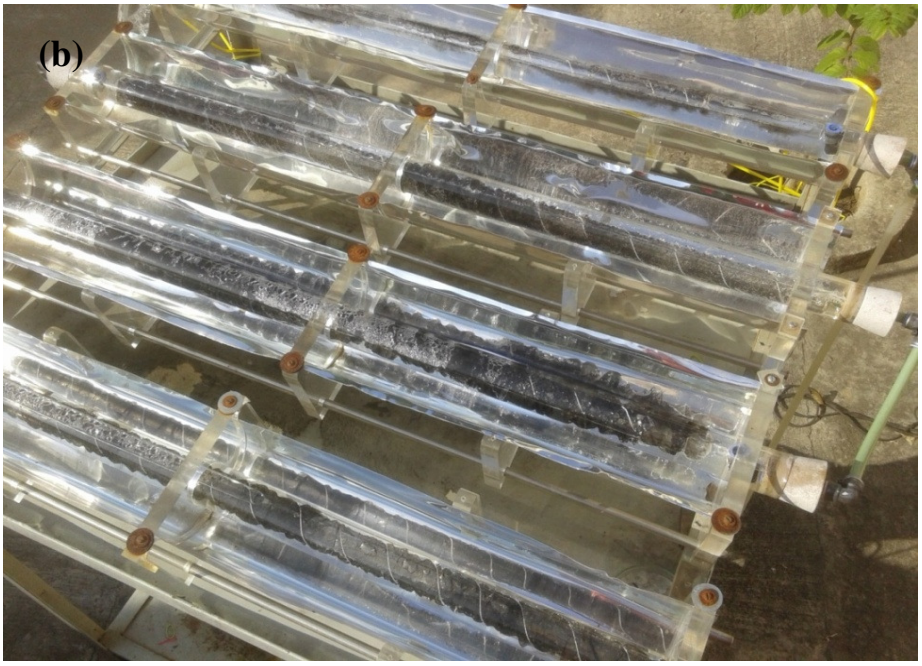

00

Fig. 1 – (a and b) Compound Parabolic Collector reactor (c) Inner tube coated with the CHIT- CNP composite film

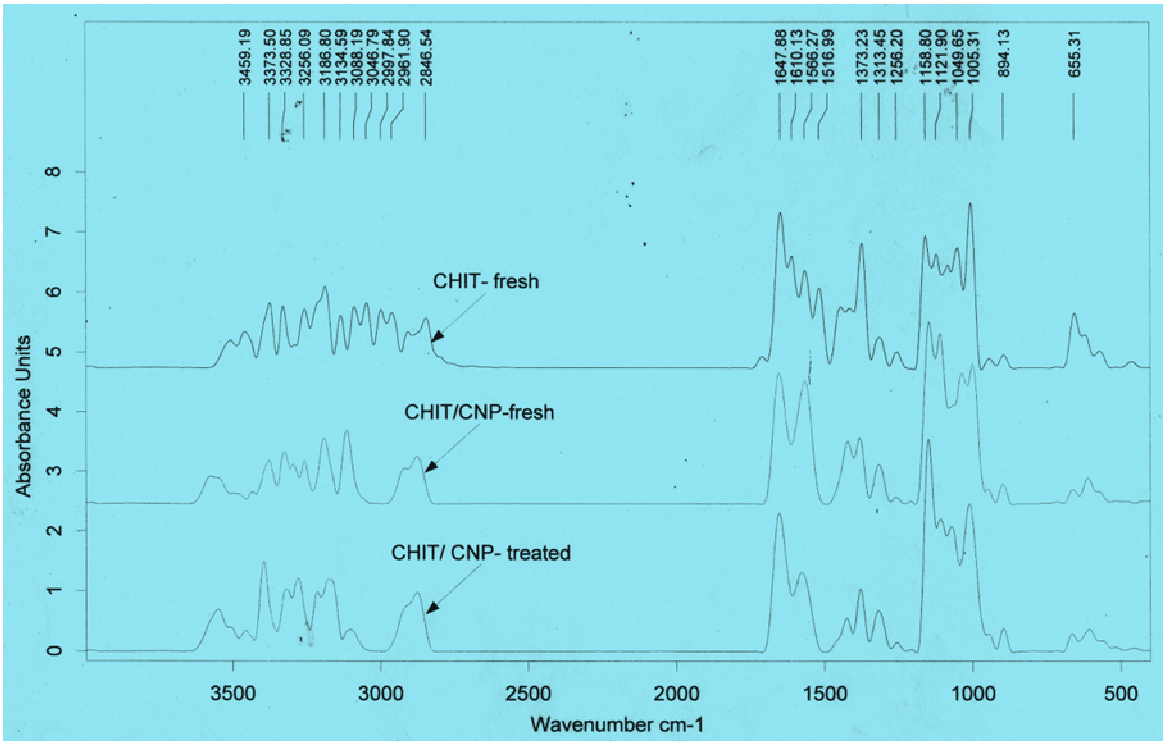

Fig. 2 - FT-IR spectra of fresh CHIT, fresh CHIT/CNP composite film and used CHIT/CNP composite film

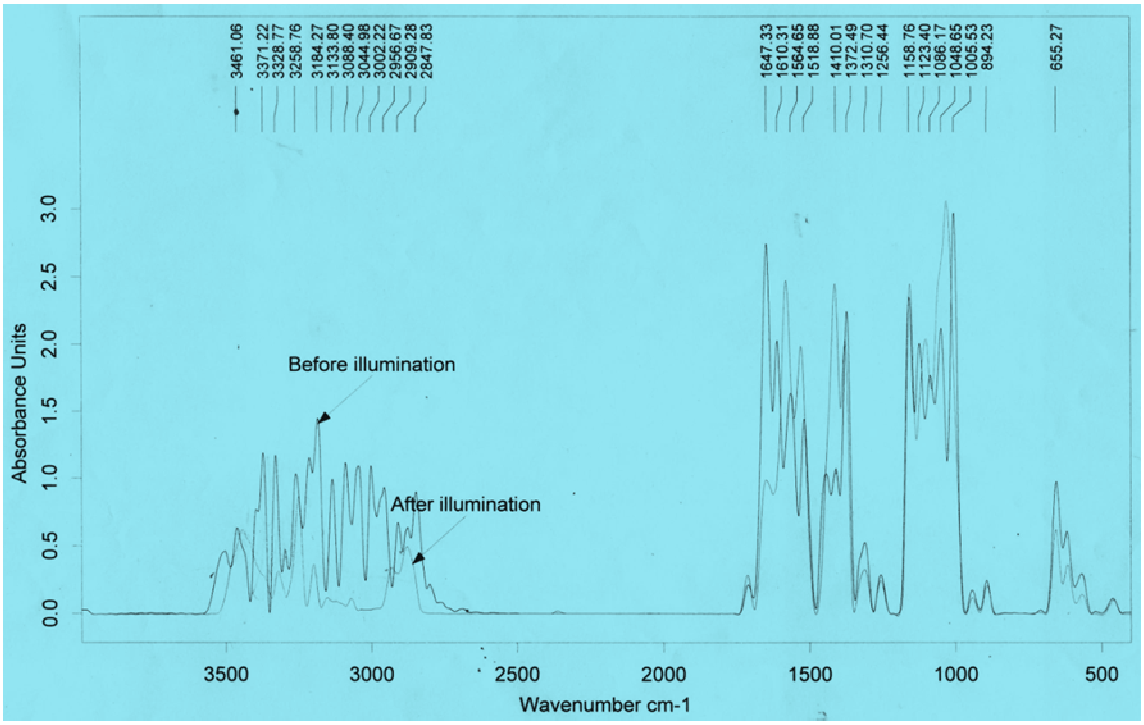

Fig. 3 - FTIR spectra of CHIT-CNP before solar illumination and after solar illumination

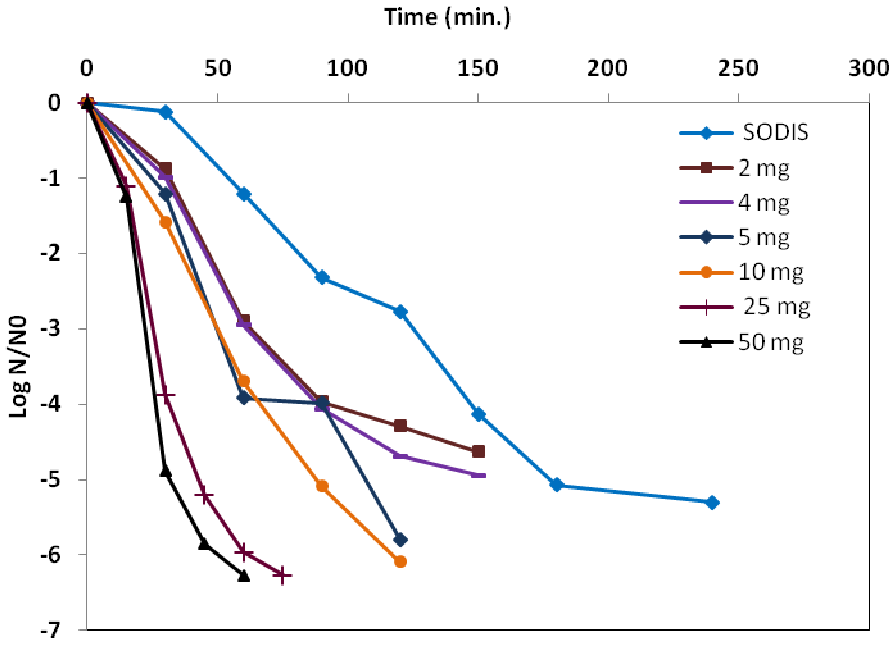

Fig. 4 – Solar disinfection (SODIS) of *E. coli* with time Vs concentration of CNP (in 50 mL volume of treatment water)

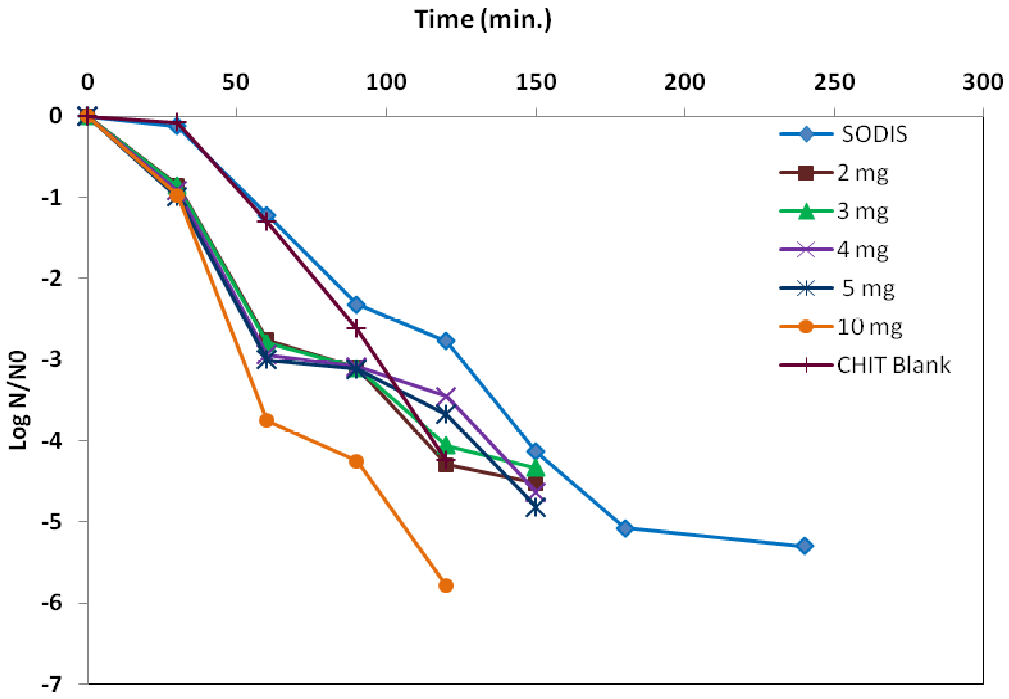

Fig. 5 – Solar disinfection (SODIS) of *E. coli* with time Vs the loading of CNP in the CHIT-CNP composite film (50 mL volume of treatment water)

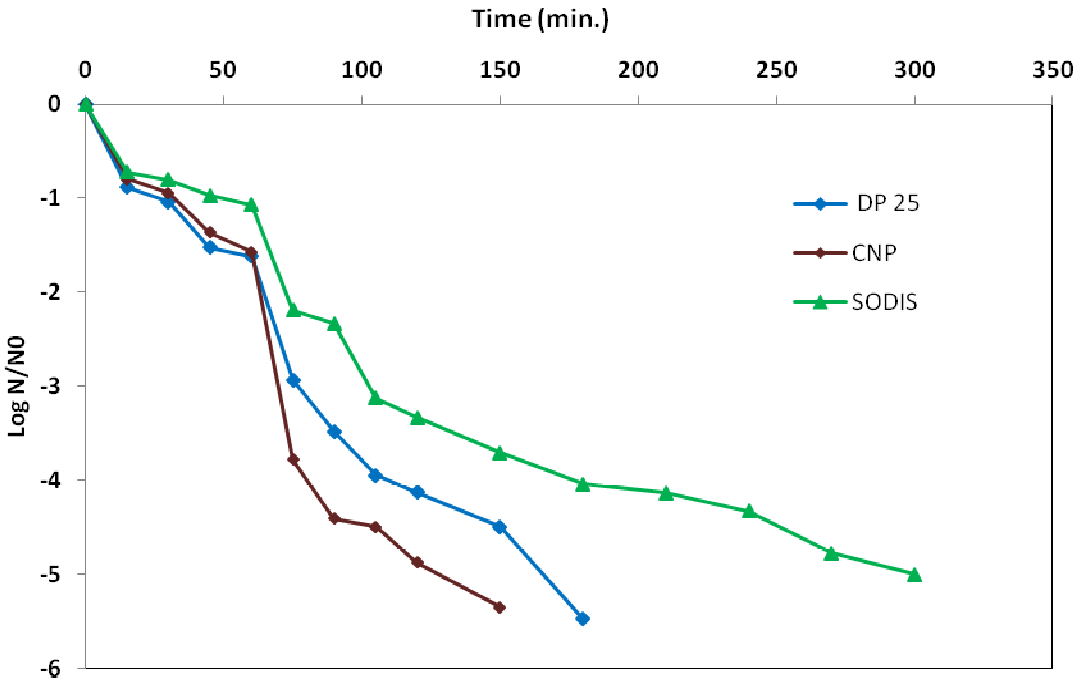

Fig. 6 – Solar disinfection (SODIS) of *E. coli*: Comparative study of CNP with DP_{25}

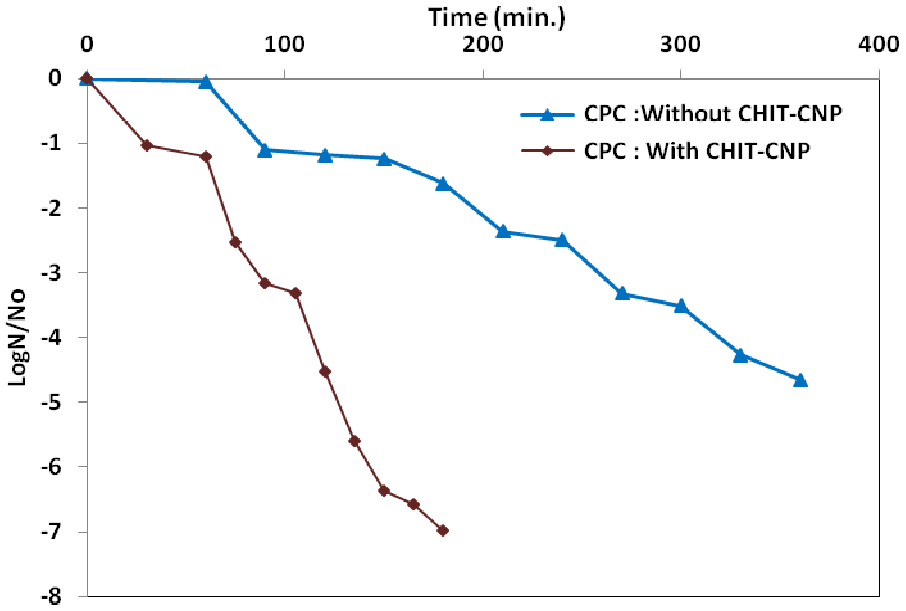

Fig. 7 – Solar disinfection (SODIS) of *E. coli* with time in the Compound Parabolic Collector (CPC) reactor: with CHIT-CNP and without CHIT-CNP (SODIS alone).